ChemPubSoc Europe

DOI: 10.1002/cphc.201601295

CHEMPHYSCHEM Articles

# Vibrational Spectrum of an Excited State and Huang–Rhys Factors by Coherent Wave Packets in Time-Resolved Fluorescence Spectroscopy

Gyeongjin Lee,[a] Junwoo Kim,[a] So Young Kim,[a] Dong Eon Kim,[b] and Taiha Joo*[a]

Coherent nuclear wave packet motions in an electronic excited state of a molecule are measured directly by time-resolved spontaneous fluorescence spectroscopy with an unprecedented time resolution by using two-photon absorption excitation and fluorescence upconversion by noncollinear sum frequency generation. With an estimated time resolution of approximately 25 fs, wave packet motions of vibrational modes up to 1600 $cm^{-1}$ are recorded for coumarin 153 in ethanol. Two-color transient absorption at 13 fs time resolution are measured to confirm the result. Vibrational displacements between the ground and excited states and Huang–Rhys factors (HRFs) are calculated by quantum mechanical methods and are compared with the experimental results. HRFs calculated by density functional theory (DFT) and time-dependent DFT reproduce the experiment adequately. This fluorescence-based method provides a unique and direct way to obtain the vibrational spectrum of a molecule in an electronic excited state and the HRFs, as well as the dynamics of excited states, and it might provide information on the structure of an excited state through the HRFs.

## 1. Introduction

The use of ultrashort pulses shorter than the period of molecular vibrations have made it feasible to generate and to probe coherent nuclear wave packets in real time. The simplest way of implementing the coherent nuclear wave packet dynamics for molecular spectroscopy is by the pump/probe transient absorption (TA), in which a short pump pulse generates nuclear wave packets in both ground and excited states, and a short probe pulse interrogates the wave packets in real time.[1–3] As ultrashort pulses short enough to generate nuclear wave packets composed of frequencies up to 3000 $cm^{-1}$ are commercially available, such experiments become practical and provide an opportunity to directly measure molecular vibrations in an electronic excited state as well as the ground state, and to investigate chemical/physical dynamics at the same time. Related techniques such as transient grating,[4] impulsive stimulated Raman scattering (ISRS),[5,6] and time-resolved ISRS[7,8] exploit nuclear wave packets. Time-resolved resonance Raman spectroscopy[9,10] and femtosecond stimulated Raman scattering (FSRS)[11–14] provide analogous information with their own advantages and disadvantages such as sensitivity to the ground-state vibrations.[15]

In TA and related methods that belong to the third and higher order nonlinear spectroscopies, nuclear wave packets are created in the electronic ground state for electronically non-resonant pump pulses, but in both electronic ground and excited states for a resonant case.[2,16] Spectral selection of the probe can differentiate the signals arising from the ground or excited pathways in favored cases.[3,17] A unique way to measure such wave packet dynamics is by time-resolved spontaneous fluorescence (TRF).[18] TRF offers several advantages compared to the nonlinear spectroscopies, including exclusive detection of the excited-state dynamics, absence of coherent artifacts, and is free from solvent intramolecular contribution. One critical difficulty of TRF is its low time resolution. To launch and to observe a vibrational wave packet, the excitation and detection time resolution should be faster than roughly half of the vibrational period. For example, it has to be around 33 fs for the detection of a 500 $cm^{-1}$ mode. The typical time resolution of femtosecond TRF apparatus using fluorescence upconversion is around 100 fs, which can measure wave packets only up to approximately 150 $cm^{-1}$, and therefore TRF is not particularly useful in this regard. We have reported a TRF apparatus showing much higher time resolution,[19,20] and also several accounts of TRF-detected excited state wave packets generated by Franck–Condon transitions,[21] internal conversion,[22] and impulsive chemical reactions.[23–25] In those studies, vibrational modes up to 500 $cm^{-1}$ have been observed by TRF.

In addition to the molecular vibrational frequencies, structural information on electronic excited states can be obtained from the amplitudes of the wave packets. A coherent nuclear wave packet leads to an oscillation of absorption and emission frequencies and therefore oscillation of time-resolved signals. The oscillation amplitude is proportional to the vibrational re-

[a] G. Lee, J. Kim, S. Y. Kim, Prof. T. Joo
Department of Chemistry
Pohang University of Science and Technology (POSTECH)
Pohang 37673 (South Korea)
E-mail: thjoo@postech.ac.kr

[b] Prof. D. E. Kim
Physics Department, Center for Attosecond Science and Technology, and Max Planck Center for Attosecond Science
Pohang University of Science and Technology (POSTECH)
Pohang 37673 (South Korea)

Supporting Information for this article can be found under: http://dx.doi.org/10.1002/cphc.201601295.

organization energy, which is proportional to the Huang–Rhys factor (HRF, *S*). Therefore, the HRF can be regarded as the selection rule for the wave-packet-assisted vibrational spectroscopies. Within the Condon approximation, $S = d^2 m\omega/2\hbar$, where *d* is the displacement between the potential energy surfaces (PESs) of the ground and excited states, and *m* and $\omega$ are the reduced mass and harmonic frequency of a vibrational mode, respectively. HRFs are directly linked to the Franck–Condon coefficients, and they are essential parameters for the descriptions of spectroscopies and dynamics of molecules. Because the displacements are directly related to the change of molecular structure, information on the structure of the excited state can be obtained from HRFs once the structure of the ground state is known, which can be obtained relatively easily.

In this report, we set out to demonstrate that the vibrational spectrum of an excited state covering the fingerprint region can indeed be obtained using TRF measurements. To this end, we have measured the TRF of coumarin 153 (C153) in ethanol with the highest time resolution by using two-photon absorption (TPA) as the pump step and gating of fluorescence by upconversion with noncollinear sum frequency generation (SFG).[20] C153 has been used extensively for studies on the static and dynamic aspects of solvation in organic solvents.[26,27] Its popularity results from the fact that its absorption and emission spectra are sensitive probes of solvent polarity as a result of a large change of dipole moment upon optical excitation. C153 is also considered as a suitable probe molecule to study solvation dynamics because of the simplicity of the $S_0$–$S_1$ transition.[27] We recorded TRF of C153 showing oscillations as high as 1600 $cm^{-1}$, arising from the vibrational wave packet motions in the $S_1$ state, although their amplitudes above 1000 $cm^{-1}$ are small due to the finite time resolution. The result was verified by a TA experiment with 13 fs resolution. Furthermore, HRFs were calculated and compared with the experiments, and numerical simulation of the TA signal by third-order nonlinear response theory was performed to determine the HRFs from the amplitudes of oscillations in TA and TRF.

## 2. Results and Discussion

### 2.1. Time-Resolved Fluorescence

The molecular structure of C153 and its absorption and fluorescence spectra peaking at 419 and 533 nm, respectively, are shown in Figure 1. Spectroscopy of C153 in the gas phase and in various solvents have been reported previously.[27–29] It is known that C153 exists in two different conformers with the julolidine group in either the *syn* or *anti* conformation, and the *syn*-conformer was determined to be the major component.[28,29] Although they show nearly the same spectral characteristics, it was observed that their vibronic spectra in the frequency region below 200 $cm^{-1}$ are significantly different.[29] Quantum mechanical calculations by density functional theory (DFT) using the B3LYP functional and the 6-31+G(d,p) basis set show that the *syn*-conformer is 110 $cm^{-1}$ below the *anti*-conformer, giving thermal populations of approximately 2:1, which is in good agreement with the previous report.[28]

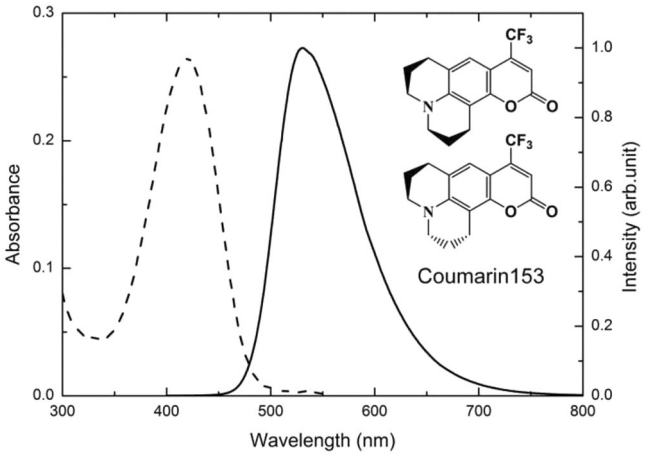


**Figure 1.** Molecular structure of coumarin 153 in the *syn* (top) or *anti* (bottom) configurations, and its absorption (dashed line) and emission (solid line) spectra in ethanol.

TRF signals measured at 490, 510, and 570 nm corresponding to the blue, center, and red part of the stationary fluorescence spectrum, respectively, are shown in Figure 2. The TRF signals at 490 and 570 nm decay and increase, respectively, originating from solvation dynamics. Because of the large Stokes shift (5100 $cm^{-1}$), the TRF signal at 510 nm, which is still on the blue side of the fluorescence spectrum, shows an initial increase. In addition to the intensity changes, the TRF signals show oscillations that persist for a few picoseconds. These oscillations must originate from the vibrational wave packet motions in the excited state of C153, because the signals arise entirely from the spontaneous fluorescence. The oscillation amplitude near the center wavelength (510 nm) is much smaller compared to those detected in the blue and red parts of the spectrum. Phases of the oscillations at the blue and red wave-

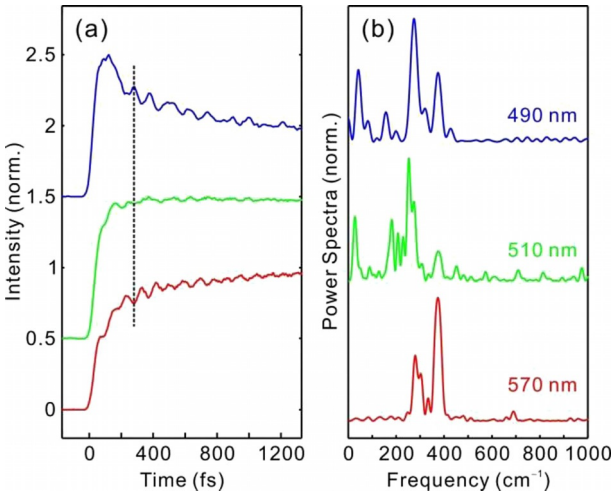


**Figure 2.** a) TRF of C153 in ethanol detected at $\lambda = 490$ (blue), 510 (green), and 570 nm (red). TRF was normalized, and the 490 and 510 nm traces are displaced vertically by 1.5 and 0.5, respectively. The dashed line indicates that the phases of the oscillations for the 490 and 570 nm signals are out of phase. b) Fourier power spectra of the residuals of the exponential fits of the TRF.

lengths are 180° out of phase. These observations indicate that the non-Condon effect is a minimal source of the intensity modulation, that is, change of the transition dipole moment upon vibration is minimal, and the intensity modulation comes from the oscillation of the fluorescence frequency over time. The TRF values were fitted to a sum of exponentials and the residuals were Fourier transformed to give the power spectra shown in Figure 2b. All the spectra show strong activities below 500 $cm^{-1}$, and the 490 nm spectrum is similar to the one reported previously.[21] Interestingly, the spectra are detection-wavelength-dependent, although the spectra at wavelengths longer than 550 nm are invariant. In particular, low-frequency vibrational modes are more prominent in the spectra detected at shorter wavelengths. Although the origin of such a spectral change is uncertain, one possibility is that excited vibrational states of low-frequency modes in the $S_1$ manifold having large HRFs might be responsible.

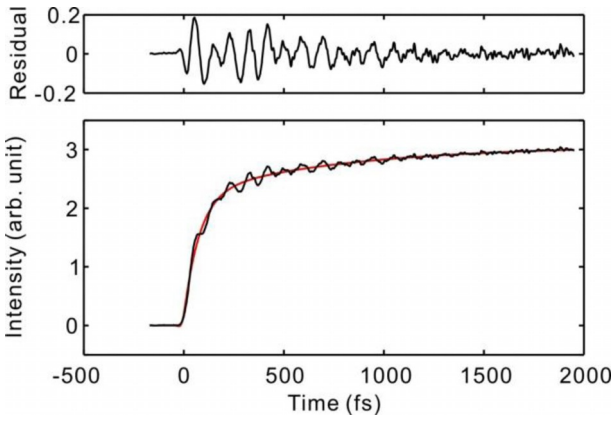


**Figure 3.** TRF of C153 in ethanol detected at $\lambda = 570$ nm. The red solid line is a fit to three exponentials. The residual (top) of the exponential fit clearly shows oscillations. A high-frequency oscillation with a period of approximately 20 fs is apparent for $t > 1000$ fs.

### 2.2. Wave Packet Spectra

Within the Condon approximation, the intensity modulation can be estimated by a simple displaced harmonic oscillator model, in which the excited-state PES is displaced by $d$ horizontally and by $\omega_{eg}$ vertically with respect to the ground-state PES. The curvatures of both the ground and excited PESs are assumed to be the same as $\omega_{vib}$. The change of the fluorescence center frequency by a wave packet motion in the excited state is [Eq. (1)]:

$$\Delta E = \hbar\Delta\omega = k_G(2d)^2/2 = 4S\hbar\omega_{vib} \quad (1)$$

where $k_G$ is the force constant in the ground state. If $S \ll 1$, the fluorescence intensity modulation for a Gaussian-shaped fluorescence spectrum detected at the half-height (HH) frequency is [Eq. (2)]:

$$\frac{\Delta I}{I_0} \cong \Delta\omega\left(\frac{dI}{d\omega}\right)_{\omega=HH} = 2\sqrt{2\ln 2}\frac{S\omega_{vib}}{\sigma} = \frac{2\sqrt{2\ln 2}}{\sigma\hbar}\lambda_{vib} \quad (2)$$

where $\sigma$ [$s^{-1}$] is the standard deviation of the Gaussian and $\lambda_{vib}$ is the vibrational reorganization energy. Therefore, the intensity modulation is directly proportional to vibrational reorganization energy, which is a product of $S$ and the vibrational energy.

The TRF acquired at 570 nm, at which the modulation is the largest, was nonlinear-least-square fitted to three exponentials of two rise time constants of 78 and 800 fs and a long nanosecond decay (Figure 3). The residual indicates that vibrational dephasing times in the $S_1$ states of molecules in liquids at room temperature ranges from a few hundred femtoseconds to a few picoseconds. The residual was Fourier transformed to give the spectrum shown in Figure 4. Because strong peaks mostly show shorter dephasing times, the $t > 1000$ fs region was also Fourier transformed to emphasize small peaks (Figure 4a, red line). The frequency spectrum obtained by the linear prediction singular value decomposition (LPSVD) method is also shown.[30–32]

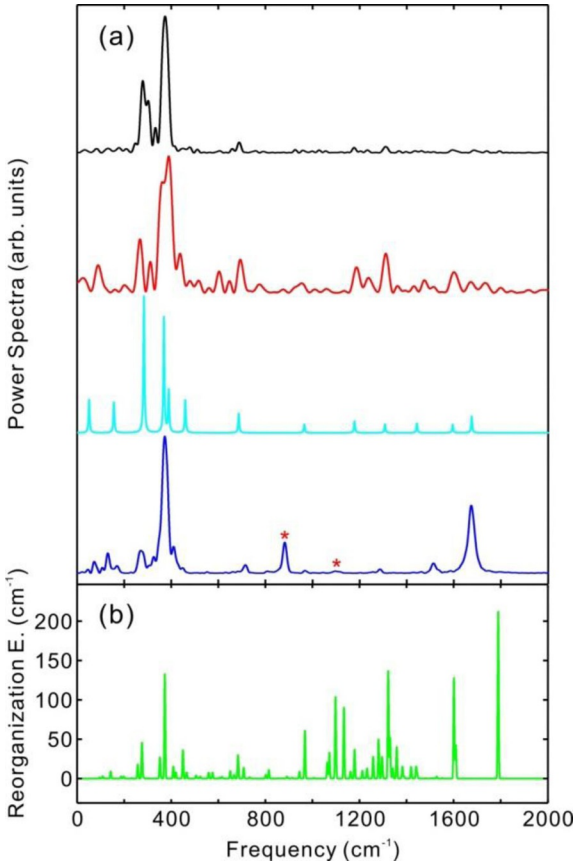


**Figure 4.** a) Fourier power spectrum (black) of the residual shown in Figure 3. The red and cyan lines are Fourier power and LPSVD spectra, respectively, for the $t > 1000$ fs region of the TRF. The blue line is the two-color TA with the pump and probe at 400 and 580 nm, respectively. The peaks marked * arise from the solvent (ethanol). b) Calculated vibrational reorganization energy for the *syn* conformer. See text for details.

In addition to the strong peaks below 500 $cm^{-1}$, Figure 4 shows that several weak peaks at high frequencies up to 1600 $cm^{-1}$ are present. Although the peak at around 1600 $cm^{-1}$ is barely observable because of the low time resolu-

tion, these small peaks appear reproducibly. In fact, the residual shown in Figure 3 shows a small-amplitude fast oscillation with a period of approximately 20 fs, which corresponds to approximately 1600 $cm^{-1}$. To confirm the result, two-color TA with the pump and probe wavelengths at 400 and 580 nm, respectively, was acquired. TA of pure ethanol (solvent) was also acquired for the reference, because pure solvent also contributes significantly by ISRS even for this non-resonant condition. The ISRS spectrum of ethanol is shown in Figure S1 in the Supporting Information. The TA signal was fitted to a sum of exponentials, and the residual was Fourier transformed to give the spectrum shown in Figure 4a (blue line). Because of the higher time resolution, a strong peak at 1675 $cm^{-1}$ appeared. We noticed, however, that the Fourier power spectrum acquired by TA is slightly different from that from TRF, and might not represent the excited state exclusively, and the ground state might contribute significantly, although the probe wavelength was tuned to the stimulated emission of C153. This point is discussed below in section 2.3.

**Table 1.** Oscillation frequencies in the TRF at 570 nm obtained by Fourier transform and LPSVD methods, and their assignments.

| Mode | Amplitude[a] | Dephasing time [fs] | Experimental frequency [$cm^{-1}$] | Calcd. frequency[b] [$cm^{-1}$] |
|---|---|---|---|---|
| | 1.2 | 550 | 51 | – |
| $\nu_8$ | 1.1 | 730 | 157 | 143 |
| $\nu_{13}$ | 5.1 | 420 | 284 | 276 |
| $\nu_{16}$ | 4.3 | 660 | 369 | 352 |
| $\nu_{18}$ | 1.6 | 1900 | 390 | 373 |
| $\nu_{22}$ | 1.2 | 780 | 460 | 450 |
| $\nu_{34}$ | 0.7 | 2100 | 687 | 684 |
| $\nu_{47}$ | 0.3 | 1900 | 965 | 968 |
| $\nu_{58}$ | 0.4 | >3000 | 1179 | 1179 |
| $\nu_{68}$ | 0.3 | >3000 | 1308 | 1322 |
| $\nu_{77}$ | 0.4 | 1500 | 1444 | 1440 |
| $\nu_{86}$ | 0.3 | >3000 | 1595 | 1601 |
| $\nu_{88}$ | 0.6 | 600 | 1676 | 1789 |

[a] Amplitude obtained from the $t > 1000$ fs region of the TRF at 570 nm. [b] Calculated frequencies of the *syn* conformer.

### 2.3. Calculation of Huang–Rhys Factors

We have calculated HRFs and vibrational reorganization energies for comparison with the vibrational spectra acquired by the time-domain experiments, and to assess the feasibility of the various theoretical methods for the proper description of the HRFs (Franck–Condon factors).[33]

First, quantum mechanical calculations were performed for C153 at several levels of theory. Molecular structures and normal modes of the ground and excited states were obtained for the two conformers by using the Gaussian 09 package.[34] A difference vector between the geometries of the ground and excited states were projected onto the normal modes of $S_1$ state to calculate the vibrational displacements and vibrational reorganization energies.[35] At the Hartree–Fock (HF) and CI-singles (CIS) level of calculations for the ground and excited states, respectively, using the 6-31+G(d,p) basis set, the calculated vibrational spectrum weighted by the vibrational reorganization energies (Tables S1 and S2) hardly matches the experimental results. DFT and TDDFT calculations for the ground and excited states, respectively, using the B3LPY functional and the 6-31+G(d,p) basis set were performed. The Duschinsky rotation matrix between the ground and $S_1$ states of C153 is mostly diagonal, indicating that change of the structure is not significant and the HRFs are mostly small. The calculated vibrational spectrum of the *syn*-conformer scaled by the vibrational reorganization energies is shown in Figure 4b (and Table S3). The corresponding spectrum of the *anti*-conformer (Figure S2 and Table S4) is nearly the same as the *syn*-conformer in the high-frequency region, but shows minor dissimilarity below 300 $cm^{-1}$. At this level of theory, the calculated vibrational spectrum scaled by the vibrational reorganization energy matches well with the spectrum obtained from TRF except in the 1000–1400 $cm^{-1}$ region. Interestingly, using a larger basis set did not further improve the match between theory and experiment. The peaks of the TRF at 570 nm ($t >$ 1000 fs) and the calculated spectrum were assigned (Table 1). Amplitude information was useful, and in most cases the vibrational assignments were straightforward. The 369 $cm^{-1}$ mode, which is seen most noticeably in the experiment, shows a large HRF. A peak at 1676 $cm^{-1}$, which appears strongly in TA, can be assigned to the C=O stretch mode at 1789 $cm^{-1}$, which also shows a large HRF in the calculation. Interestingly, calculations show that there are many modes with large HRFs in the 1000–1400 $cm^{-1}$ region, whereas the spectra from experiment are mostly silent. However, the small peaks in the 600–1600 $cm^{-1}$ region can be readily assigned only to the modes that show large HRFs in the calculation.

The frequencies obtained from the TA experiment are slightly different from those from TRF. We suspect that the wave packets created in the ground state contribute to the vibrational spectrum. We calculated the vibrational spectrum of the ground state weighted by the vibrational reorganization energies by projecting the difference vector between the geometries of the ground and excited states onto the normal modes of the ground state (Figure S2 and Tables S3 and S4). The ground spectrum obtained in this way is analogous to the resonance Raman spectrum. Although it is inconclusive, several peaks from TA can be assigned to the vibrational modes in the ground state calculated in this way. For example, two peaks at 1288 and 1510 $cm^{-1}$ present in the spectrum from TA can be assigned to the 1288 ($\nu_{65}$) and 1514 ($\nu_{83}$) $cm^{-1}$ modes in the ground state that show large HRFs, whereas these modes show small HRFs in the excited state.

We also compared the experimental results to the molecular dynamics simulations under the interpolated PES reported by Park and Rhee.[36] The solvent response functions of C153 were calculated from the molecular dynamics simulation. After subtracting the fitted multi-exponential components from the solvent response functions, the remaining oscillations were analyzed to obtain the spectrum of vibrational wave packet motion.[36] There are relatively large discrepancies between the experiment and theory. We suggest that the quality of the

match might depend on the quality of the quantum mechanical calculation part, implying that solvent response does not contribute much to the excited state vibrational spectrum, as predicted from the separation of the intramolecular nuclear coordinates from the solvent coordinate, whereas electronic states are strongly coupled to the solvent nuclear coordinates.

### 2.4. Time-Resolved Signal Calculation

It was gratifying to observe nuclear wave packet motions in the excited state as high as 1600 $cm^{-1}$ by TRF. However, the oscillation amplitudes at high frequencies are attenuated significantly by the finite time resolution. The attenuation factor can be estimated from a simple convolution of a Gaussian instrument response function (IRF) and a sinusoid. An oscillation is attenuated by $\exp(-\omega^2\sigma^2/2)$, where $\omega$ is the oscillation frequency and $\sigma$ is the standard deviation of the Gaussian. Because the IRF width of the TA experiment was 13 fs, the vibrational modes at 1600 and 3000 $cm^{-1}$ are attenuated by factors of 4 and 130, respectively. However, we routinely observed C–H stretching vibrations at approximately 3000 $cm^{-1}$ with significant amplitude in a TA measurement at this time resolution, provided that the spectral width of the pump pulse is wide enough to create the wave packet at 3000 $cm^{-1}$. It is important to obtain the attenuation factor of an oscillation amplitude for the actual experimental condition to determine the HRF and the Franck–Condon factor. We calculated TA signals at different pulse durations to show the validity of the estimation of the oscillation amplitude by $\exp(-\omega^2\sigma^2/2)$ and to evaluate the attenuation factor in the actual experimental conditions.

A TA signal can be calculated by using the third-order nonlinear response theory starting from the transition frequency correlation function [Eq. (3)]:[4,16]

$$M(t) = \frac{\langle \delta\omega_e(0)\delta\omega_e(t)\rangle}{\langle \delta\omega_e^2\rangle} \quad (3)$$

where $\delta\omega_e(t) = \langle\omega_e\rangle - \omega_e(t)$. Here, $\langle\omega_e\rangle$ is the average electronic transition frequency, $\omega_e(t)$ is the transition frequency at time $t$, and the brackets denote ensemble average. A TA signal depends on the pulse duration, electronic dephasing dynamics of the system, and the vibrational frequency. A TRF signal can also be calculated using the third-order nonlinear response theory.[16,37] For the $M(t)$ function for C153 in ethanol, we used the solvation parameters reported previously [Eq. (4)]:[21,26]

$$\langle \delta\omega_e^2\rangle M(t) = \Delta_{Gau}^2 \exp[-(t/\tau_{Gau})^2] + \Delta_{exp}^2 \sum_{i=1}^{4} A_i \exp(-t/\tau_i) \quad (4)$$

where values of $\tau_i$ are 120 fs and 5, 30, and 100 ps, and $A_i$ are 0.2, 0.2, 0.3, and 0.3, respectively. The Gaussian component was included to account for the fact that the fluorescence spectra at $t=0$, measured at 40 fs resolution, is maximum at 490 nm.[21] The coupling strength between the electronic transition and the solvent nuclear coordinate, $\Delta_{Gau}$ and $\Delta_{exp}$, are 940 and 470 $cm^{-1}$, respectively. Absorption and fluorescence spectra calculated with these parameters show that the widths are 2450 $cm^{-1}$, excluding the vibronic structure, and the Stokes shift is 5070 $cm^{-1}$; these are consistent with the spectra shown in Figure 1. Details of the parameters do not greatly affect the final results. The amplitudes, frequencies, and phases of the oscillation in a calculated TA signal were obtained by using the LPSVD method.

Figure 5 shows the normalized modulation amplitude $\Delta I/I_0$ as a function of vibrational frequency for three different pulse durations. The actual value of the modulation depth at low frequency, which the experimental time resolution does not affect, is 0.15 (9.2 fs pulse width) for the vibrational reorganization energies of 95 $cm^{-1}$. The estimated value from the simple displaced harmonic oscillator model is 0.215, and matches satisfactorily. Cross-correlation of 13 fs gives a pulse duration of 9.2 fs, assuming the same width for the pump and probe pulses. The attenuation factor of the 1600 $cm^{-1}$ mode for a pulse duration of 9.2 fs is 2.2, which is also in good agreement. For a pulse duration of 9.2 fs, the 3000 $cm^{-1}$ mode is attenuated by a factor of 40, smaller than the simple estimation, and should be readily observable. The attenuation factor for the TRF should be between the attenuation factors for the pulse widths of 14.4 and 20, that is, 8.6 and 130. Therefore, the 1600 $cm^{-1}$ mode should be observable, as demonstrated in this work. Considering that the relative amplitude of the 1675 $cm^{-1}$ peak with respect to the 375 $cm^{-1}$ peak in the spectrum obtained from TA is 0.6 and that the value from TRF is approximately 10, the experimental attenuation factor can be estimated to be around 20, which is within the range of estimation. The actual time resolution of the TRF experiment, therefore, should be around 25 fs. Because important vibrational modes usually occur below 1700 $cm^{-1}$, a time resolution of TRF close to 20 fs is desirable for the investigation of chemical problems.

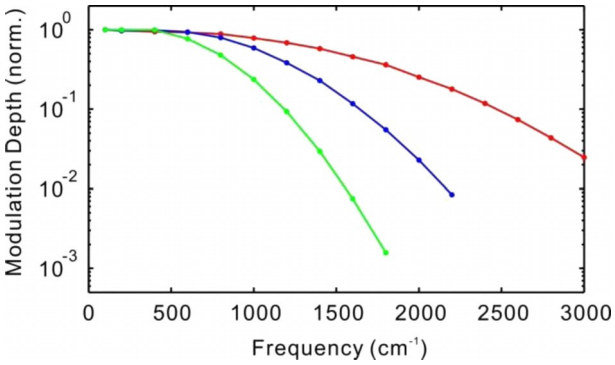


**Figure 5.** Normalized modulation depth (oscillation amplitude) as a function of frequency in the calculated TA signal for pulse durations of 9.2 (red), 14.1 (blue), and 20 fs (green).

## 3. Conclusions

Nuclear wave packet motion in an excited state can be observed directly in the time domain by time-resolved spontane-

ous fluorescence measurements. By using TPA electronic excitation, noncollinear sum frequency generation as a fluorescence upconversion process, and careful optimization of the apparatus, we were able to observe wave packet motions for vibrational modes as high as 1600 $cm^{-1}$ in the excited state of C153 in ethanol by TRF. Huang–Rhys factors were calculated by the quantum mechanical methods, and matches well with the vibrational modes observed by TRF. Interestingly, however, vibrational modes in the 1000–1400 $cm^{-1}$ region were mostly silent experimentally but showed large Huang–Rhys factors in the calculation. The time resolution estimated by the amplitude of the wave packet motion was around 25 fs. Even at this unprecedented high resolution, the oscillation amplitude for the 1600 $cm^{-1}$ mode is still heavily attenuated due to the finite time resolution of the TRF apparatus. The vibrational spectrum obtained in this way is weighted by the vibrational reorganization energies, which should give information on the change of the molecular structures from the ground to the excited state. Because the molecular structure of a ground state is easily accessible experimentally and theoretically, this vibrational spectroscopy from coherent wave packets should be a powerful technique in molecular spectroscopic and molecular dynamics studies.

## Experimental Section

### Time-resolved Fluorescence

Femtosecond TRF was performed by a TPA-excited fluorescence upconversion technique described elsewhere.[20] In a typical fluorescence up-conversion experiment, a pump pulse was prepared by the second harmonic generation (SHG) of the pulses from a mode-locked Ti:sapphire laser, the duration of which is significantly longer than the fundamental due to the group velocity mismatch (GVM). We used TPA excitation and noncollinear SFG for the fluorescence upconversion to achieve higher time resolution by circumventing pulse broadening in the SHG process and GVM in SFG. In addition, excitation by TPA effectively reduces the duration of pumping by $\sqrt{2}$ compared to the actual pump pulse width. A thin BBO crystal ($\approx$10 μm) can also be used to obtain a pump pulse shorter than the fundamental, although the SHG efficiency would be too small to perform the TRF measurement. The femtosecond light source was a in-house-built cavity-dumped Ti:sapphire oscillator pumped by a frequency-doubled Nd:$YVO_4$ laser (Verdi, Coherent Inc., Santa Clara, USA). Cavity-dumped output centered at 800 nm at the repetition rate of 760 kHz was split into two by a beam splitter, and used as pump and gate pulses. Group velocity dispersion (GVD) of the pump and gate pulses was compensated by negative GVD mirrors (Layertec GmbH, Mellingen, Germany). The pump beam was focused tightly into a sample solution by using a lens of focal length 1.9 cm. Fluorescence was collected by a reflective microscope objective lens, and mixed with the gate pulse in a 100 or 300 μm thick β-barium borate (BBO) crystal. To achieve the best time resolution, we carefully minimized the GVD, GVM, and phase-front mismatch in the SFG process. Polarization of the pump pulse was rotated with respect to the gate by 54.7° using an achromatic half-waveplate. The upconverted signal was dispersed by a double monochromator and detected by a photomultiplier tube and gated photon counter. The cross-correlation between the gate and scattered 800 nm pump pulses was 30 fs (full width at half-maximum). Actual instrument response of the TRF signal, however, should be better because of the shorter pump step by TPA.

### Transient Absorption

The light source was based on a commercial carrier envelope phase-stabilized multipass amplifier (Femtopower, Femtolaser Inc., Vienna, Austria) operating at 3 kHz repetition rate, nominal center wavelength of 800 nm, and pulse duration of 25 fs. The output was focused to a gas-filled hollow-core fiber to generate a continuum, which was compressed by several pairs of negative GVD mirrors. A broadband pump pulse centered at 400 nm was generated by SHG of the continuum in a thin BBO crystal of 20 μm thickness. The spectral width of the pump pulses was greater than 50 nm, and more than sufficient to create the wave packet of the C–H stretching vibrations at 3000 $cm^{-1}$. Pulse compression of the SHG and the continuum were achieved by using a series of negative GVD mirror pairs and wedge prism pairs. A beam reflected at one of the wedge prisms was used as a probe. Pulse energies of the pump and probe were attenuated to 10 nJ and $<$100 pJ, respectively, to avoid higher order processes. The cross-correlation between the pump and probe was 13 fs, and it was sufficiently high to resolve oscillation frequencies higher than 3000 $cm^{-1}$. A TA signal of neat ethanol was measured as a reference, Fourier transform of which yielded significant intensity around 3000 $cm^{-1}$ arising from the C–H stretching vibrations.

### Sample Preparation

Coumarin 153 was purchased from Lambda Physik (Göttingen, Germany) and used without purification. A solution in ethanol was prepared at an absorbance of approximately 0.3 in a 200 μm pathlength flow cell and was flown by a gear pump. All experiments were performed at ambient temperature.

## *Acknowledgements*

*This work was supported by the Global Research Laboratory Program (2009-00439) of the National Research Foundation of Korea (NRF) grant funded by the Korean government (MSIP).*

## Conflict of Interest

*The authors declare no conflict of interest.*

**Keywords:** coumarin · Franck–Condon factors · Huang–Rhys factors · nuclear wave packets · time-resolved fluorescence

[1] M. J. Rosker, F. W. Wise, C. L. Tang, *Phys. Rev. Lett.* **1986**, *57*, 321 – 324.
[2] I. A. Walmsley, M. Mitsunaga, C. L. Tang, *Phys. Rev. A* **1988**, *38*, 4681 – 4689.
[3] W. T. Pollard, S.-Y. Lee, R. A. Mathies, *J. Chem. Phys.* **1990**, *92*, 4012 – 4029.
[4] T. Joo, Y. W. Jia, J. Y. Yu, M. J. Lang, G. R. Fleming, *J. Chem. Phys.* **1996**, *104*, 6089 – 6108.
[5] P. Voehringer, N. F. Scherer, *J. Phys. Chem.* **1995**, *99*, 2684 – 2695.
[6] T. Joo, M. A. Dugan, A. C. Albrecht, *Chem. Phys. Lett.* **1991**, *177*, 4 – 10.
[7] S. Fujiyoshi, S. Takeuchi, T. Tahara, *J. Phys. Chem. A* **2003**, *107*, 494 – 500.
[8] H. Kuramochi, S. Takeuchi, T. Tahara, *Rev. Sci. Instrum.* **2016**, *87*, 043107.
[9] H. Hamaguchi, T. L. Gustafson, *Annu. Rev. Phys. Chem.* **1994**, *45*, 593 – 622.

[10] Y. Mizutani, Y. Uesugi, T. Kitagawa, *J. Chem. Phys.* **1999**, *111*, 8950 – 8962.
[11] M. Yoshizawa, M. Kurosawa, *Phys. Rev. A* **1999**, *61*, 013808.
[12] P. Kukura, D. W. McCamant, S. Yoon, D. B. Wandschneider, R. A. Mathies, *Science* **2005**, *310*, 1006 – 1009.
[13] C. Fang, R. R. Frontiera, R. Tran, R. A. Mathies, *Nature* **2009**, *462*, 200 – 204.
[14] S. Y. Lee, D. H. Zhang, D. W. McCamant, P. Kukura, R. A. Mathies, *J. Chem. Phys.* **2004**, *121*, 3632 – 3642.
[15] K. Niu, B. Zhao, Z. Sun, S.-Y. Lee, *J. Chem. Phys.* **2010**, *132*, 084510.
[16] S. Mukamel, *Principles of Nonlinear Optical Spectroscopy*, Oxford University Press, New York, **1999**.
[17] J. S. Park, T. Joo, *J. Chem. Phys.* **2002**, *116*, 10801 – 10808.
[18] J. Conyard, K. Addison, I. A. Heisler, A. Cnossen, W. R. Browne, B. L. Feringa, S. R. Meech, *Nat. Chem.* **2012**, *4*, 547 – 551.
[19] H. Rhee, T. Joo, *Opt. Lett.* **2005**, *30*, 96 – 98.
[20] C. H. Kim, T. Joo, *Opt. Express* **2008**, *16*, 20742 – 20747.
[21] I. Eom, T. Joo, *J. Chem. Phys.* **2009**, *131*, 244507.
[22] S. Y. Kim, T. Joo, *J. Phys. Chem. Lett.* **2015**, *6*, 2993 – 2998.
[23] C. H. Kim, T. Joo, *Phys. Chem. Chem. Phys.* **2009**, *11*, 10266 – 10269.
[24] C.-C. Hsieh, P.-T. Chou, C.-W. Shih, W.-T. Chuang, M.-W. Chung, J. Lee, T. Joo, *J. Am. Chem. Soc.* **2011**, *133*, 2932 – 2943.
[25] S. Y. Kim, C. H. Kim, M. Park, K. C. Ko, J. Y. Lee, T. Joo, *J. Phys. Chem. Lett.* **2012**, *3*, 2761 – 2766.
[26] M. L. Horng, J. A. Gardecki, A. Papazyan, M. Maroncelli, *J. Phys. Chem.* **1995**, *99*, 17311 – 17337.
[27] J. E. Lewis, M. Maroncelli, *Chem. Phys. Lett.* **1998**, *282*, 197 – 203.
[28] A. Mühlpfordt, R. Schanz, N. P. Ernsting, V. Farztdinov, S. Grimme, *Phys. Chem. Chem. Phys.* **1999**, *1*, 3209 – 3218.
[29] B. A. Pryor, P. M. Palmer, Y. Chen, M. R. Topp, *Chem. Phys. Lett.* **1999**, *299*, 536 – 544.
[30] I. Eom, E. Yoon, S.-H. Baik, Y.-S. Lim, T. Joo, *Opt. Express* **2014**, *22*, 30512 – 30519.
[31] A. E. Johnson, A. B. Myers, *J. Chem. Phys.* **1996**, *104*, 2497 – 2507.
[32] G. L. Millhauser, J. H. Freed, *J. Chem. Phys.* **1986**, *85*, 63 – 67.
[33] I. Pugliesi, K. Müller-Dethlefs, *J. Phys. Chem. A* **2006**, *110*, 4657 – 4667.
[34] Gaussian 09, Revision B.01, M. J. Frisch, G. W. Trucks, H. B. Schlegel, G. E. Scuseria, M. A. Robb, J. R. Cheeseman, G. Scalmani, V. Barone, B. Mennucci, G. A. Petersson, H. Nakatsuji, M. Caricato, X. Li, H. P. Hratchian, A. F. Izmaylov, J. Bloino, G. Zheng, J. L. Sonnenberg, M. Hada, M. Ehara, K. Toyota, R. Fukuda, J. Hasegawa, M. Ishida, T. Nakajima, Y. Honda, O. Kitao, H. Nakai, T. Vreven, J. A. Montgomery, J. E. Peralta, F. Ogliaro, M. Bearpark, J. J. Heyd, E. Brothers, K. N. Kudin, V. N. Staroverov, R. Kobayashi, J. Normand, K. Raghavachari, A. Rendell, J. C. Burant, S. S. Iyengar, J. Tomasi, M. Cossi, N. Rega, J. M. Millam, M. Klene, J. E. Knox, J. B. Cross, V. Bakken, C. Adamo, J. Jaramillo, R. Gomperts, R. E. Stratmann, O. Yazyev, A. J. Austin, R. Cammi, C. Pomelli, J. W. Ochterski, R. L. Martin, K. Morokuma, V. G. Zakrzewski, G. A. Voth, P. Salvador, J. J. Dannenberg, S. Dapprich, A. D. Daniels, Ö. Farkas, J. B. Foresman, J. V. Ortiz, J. Cioslowski, D. J. Fox, Gaussian, Inc, Wallingford CT, **2009**.
[35] J. R. Reimers, *J. Chem. Phys.* **2001**, *115*, 9103 – 9109.
[36] J. W. Park, H. W. Kim, C.-i. Song, Y. M. Rhee, *J. Chem. Phys.* **2011**, *135*, 014107.
[37] D. Lee, A. C. Albrecht in *Advances in Infrared and Raman Spectroscopy, Vol. 12* (Eds.: R. J. H. Clark, R. E. Hester), Wiley Heyden, New York, **1985**, pp. 179 – 213.

Manuscript received: November 23, 2016
Revised: January 5, 2017
Accepted Article published: January 10, 2017
Final Article published: February 2, 2017